

Temperature-dependent resistance of a finite one-dimensional Josephson junction array

Klas Engström and Jari M. Kinaret

*Department of Applied Physics, Chalmers University of Technology and Göteborg University
SE-412 96 Göteborg, Sweden
E-mail: klase@fy.chalmers.se*

Received August 27, 2001

We study theoretically the temperature and array-length dependences of the resistance of a finite one-dimensional array of Josephson junctions. We use both analytic approximations and numerical simulations, and conclude that within the self-charging model, all finite arrays are resistive in the low-temperature limit. A heuristic analysis shows qualitative agreement with resistance obtained from Monte Carlo simulations, establishing a connection between resistance and the occurrence of vortices in the corresponding $1 + 1D$ XY-model. We compare our results with recent experiments and conclude that while the self-charging model reproduces some of the experimental observations, it underestimates the superconducting tendencies in the experimental structures.

PACS: **74.50.+r**, 73.23.Hk, 74.25.Fy

1. Introduction

The one-dimensional Josephson junction array is a prime example of a system exhibiting a zero-temperature superconductor–insulator quantum phase transition (QPT). Various investigations of the system, using different approximations for the capacitance matrix and dissipation [1–5], have revealed a rich phase diagram. Most theoretical studies so far have focused on the limit of infinite system size and zero temperature. This sequence of limits per definition excludes finite size effects and is therefore mathematically simple, lending itself to standard quantum statistical mechanics treatments. Recent experiments [6] on chains consisting of 63 to 255 junctions show results suggestive of the predicted infinite-system QPT. However, the measured array resistances were found to depend both on the number of junctions and the temperature in a non-obvious fashion. In particular, the resistance of a given array varied non-monotonically as a function of temperature and exhibited regions of pronounced quasi-reentrant insulating and superconducting behaviors. In this paper we investigate this thus far unexplained non-monotonicity in terms of a familiar path integral treatment of the problem. We also discuss the effects of finite chain length on both

sides of the nominal superconductor–insulator transition point.

Finite one-dimensional arrays of Josephson junctions have previously been analyzed by Inoue et al. [3], who discussed the zero temperature behavior in terms of real-time phase slips. They calculated the length dependence of the crossover between low- and high-resistance regimes, and found qualitative agreement with the measurements of Chow et al.. Explicit resistance values were calculated only in the $N \rightarrow \infty$ limit though. Our results agree with those of Inoue et al. in that we also find a resistive low-temperature behavior, but in contrast to the earlier work we also analyze the finite-temperature behavior of the array.

The paper is organized as follows: Section 2 presents the model. In Sec. 3 we present a qualitative analysis of the dependence of the linear-response resistance on parameters such as system length, temperature, and Josephson coupling. The qualitative results are put on a firmer footing in Sec. 4, in which we present Monte Carlo data in support of the proceeding arguments and make comparison with existing experimental data. Conclusions and discussion follow in Sec. 5.

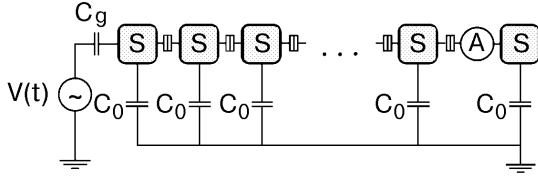


Fig. 1. Regions marked with S denote superconducting grains, separated by tunnel junctions. Each grain is capacitively coupled to a ground plane through a capacitance C_0 . The response to the externally applied voltage $V(t)$ is measured by a fictitious ideal current-meter A between any two grains. The total number of Cooper pairs on the array is conserved.

2. Model

Among the simplest models incorporating both charging and Josephson effects is the self-charging model [1] in which only the self-capacitance C_0 of the individual islands is taken into account (Fig. 1). The Hamiltonian in this case takes the simple form

$$H = \sum_i \left[E_C \hat{n}_i^2 - 2E_J \cos(\hat{\varphi}_{i+1} - \hat{\varphi}_i) \right],$$

where $E_C = (2e)^2/(2C_0)$ is the charging energy; E_J is the Josephson energy, and $\hat{\varphi}_i$ is the phase conjugate to the number of Cooper pairs \hat{n}_i , on grain i .

Quite generally, the behavior of a quantum D -dimensional system can be understood in terms of a $D + 1$ -dimensional classical system, where the extra dimension is imaginary time [7]. As shown by Bradley and Doniach [1], the self-charging model maps onto a 2D XY -model on a cylindrical [8] lattice of length N and circumference $N_\tau \propto T^{-1}$ in the imaginary-time (τ) direction. The equivalent coupling constant of the XY -model is given by $K \equiv \sqrt{E_J/E_C}$. Hence, the QPT is of the Kosterlitz–Thouless–Berezinskii (KTB) type [9], corresponding to the unbinding of vortices in the 2D spin field $\varphi(x, \tau)$ – in real-time formalism the vortices correspond to phase slips [3]. Note that the vortices that appear in the analysis of 2D Josephson arrays are real vortices of the field $\varphi(x, y)$ and hence quite different from the structures that we focus on, which are vortices of $\varphi(x, \tau)$ or phase slips of $\varphi(x, t)$.

The step size $\Delta\tau$ in the imaginary time direction is so chosen that the resulting XY -model is isotropic. This approximation is valid provided that the characteristic time scale for variations of $\varphi(x, \tau)$ is slower than $\Delta\tau$, i.e., provided that K is not too small.

The current $I(x, t)$ arising as a response to an applied voltage $V(t)$ can be obtained by standard linear response formalism [10]. In the 2D XY -model this requires a knowledge of spin–spin correlations.

3. Qualitative analysis

3.1. Introduction

It is well known [1,7] that the appearance of resistance in Josephson junction arrays can be associated with isolated vortices in the two-dimensional XY -model. However, the quantitative connection between the number of isolated vortices and resistance R is not clear, but the resistance is believed to be a monotonic function of the number of independent vortices [7]. In this Section we use this connection to determine the qualitative temperature and system size dependences of R for finite one-dimensional arrays of Josephson junctions.

Since the vortex excitations and spin waves decouple in the 2D XY -model, we can write the

partition function as $Z = Z_{sw} \sum_{n=0}^{\infty} Z_n$, where Z_{sw} is

the spin-wave contribution and Z_n is the contribution from a spin configuration with n vortices ($Z_0 = 1$). In general it is unclear which of the vortices should be classified as isolated (and hence contribute significantly to the resistance) and which of them belong to closely bound vortex-anti-vortex pairs. However, we know that in the limit of large K the free energy cost of creating an isolated vortex is very high, and most vortices occur in vorticity-neutral pairs, and we can therefore approximate $Z_{2n+1} \approx Z_1 Z_{2n}$. Hence, for large K , the number of unbound vortices is approximately

$$\langle N_V \rangle \approx \left(\sum_{n=1}^{\infty} Z_1 Z_{2n} \right) / \left(\sum_{n=0}^{\infty} Z_n \right) = Z_1 / (1 + Z_1) \approx Z_1.$$

In the opposite limit of small K all vortices are nearly

independent, and $\langle N_V \rangle \approx \left(\sum_{n=0}^{\infty} n Z_n \right) / \left(\sum_{n=0}^{\infty} Z_n \right)$. In this

limit the vortex gas can be described as a collection of indistinguishable particles, so that $Z_n = (1/n!) Z_1^n$, and we again find $\langle N_V \rangle \approx Z_1$. Consequently, we use Z_1 as an estimate for the number of free vortices in the system.

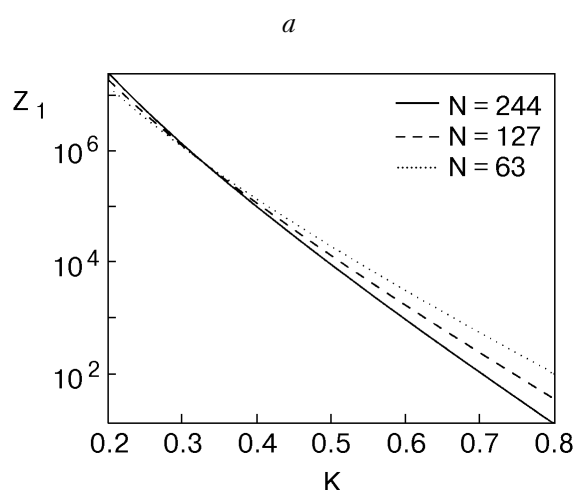
The partition function $Z_1 = \int \mathcal{D}\varphi(x, t) e^{-H[\varphi]}$ (where the integration extends over single-vortex configurations $\varphi(x, t)$ only) we estimate by calcu-

lating the typical energy E_{typ} of a single vortex, and by multiplying $e^{-E_{\text{typ}}}$ by an entropic factor which gives the number of possible places where a vortex may appear. This argument by Kosterlitz and Thouless [9,11] demonstrates the existence of a phase transition in an infinite 2D XY -model, and for the present purposes we extend it to a cylindrical geometry. A typical vortex configuration, centered at (x_0, τ_0) , that satisfies periodic boundary conditions in the imaginary time direction is $|\tau| < N_\tau/2$

$$\varphi(x, \tau) = \arctan \left[\coth \left(\frac{\pi}{N_\tau} (x - x_0) \right) \tan \left(\frac{\pi}{N_\tau} \tau \right) \right] + \frac{\pi}{N_\tau} \tau + \pi \operatorname{sgn}(\tau) [1 - \theta(x - x_0)] ,$$

where we close the principal branch of \arctan and where the last two terms were added to guarantee that the spin directions end up in the proper quadrant [12]. Using a continuum approximation for the energy E_{typ} and taking the entropy S_{typ} to be $\sim \ln NN_\tau$, we find, apart from uninteresting constants, a typical free energy

$$F = E_{\text{typ}} - S_{\text{typ}} \approx K \pi \left\{ \ln \left[\frac{\sinh(\pi(N/N_\tau))}{\sinh(\pi(2/N_\tau))} \right] - \frac{\pi}{2} \frac{N}{N_\tau} \right\} - \ln(NN_\tau) . \quad (1)$$



In the following two Sections we investigate the dependence of F on the chain length N and temperature N_τ^{-1} .

In order to facilitate a direct comparison with experiments [6], we fix the charging energy to $E_C = 500 \mu\text{eV}$ and vary K by varying E_J . Experimentally, E_J can be tuned by means of an external magnetic field. For simplicity, we ignore the temperature dependence of E_J .

3.2. Results

Keeping the aspect ratio $A \equiv N_\tau/N \propto (NT)^{-1}$ fixed in Eq. (1) and sending N to infinity, we get

$$F \approx (\pi K - 2) \ln N + O(N^{-1}) + \text{const}$$

and we recover the familiar infinite-system result for a continuum: a phase transition occurs at $K = K_{KTB} \equiv 2/\pi$. Note, however, that the limits $N \rightarrow \infty$ and $T \rightarrow 0$ do not commute. The experimentally relevant limit where N is kept fixed as T is lowered is

$$F \approx (K\pi - 1) \ln N - \ln N_\tau - K \frac{\pi^2}{2} \frac{N}{N_\tau} + \text{const} \xrightarrow{T \rightarrow 0} -\infty . \quad (2)$$

Hence, in the limit of low temperatures, free vortices are always present in a finite array, suggesting that the low-temperature behavior of finite arrays is insulating rather than superconducting. This is an immediate consequence of the periodic boundary conditions in the imaginary-time direc-

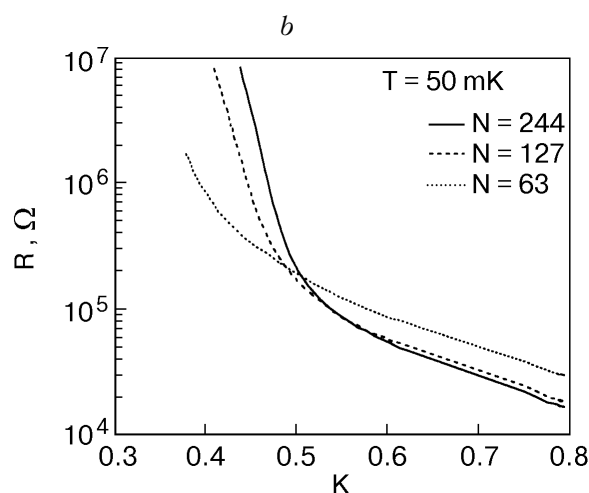


Fig. 2. Variation of Z_1 with K for different chain lengths N at a very low temperature. Note that quantity on the y axis is not the actual resistance, but the number of free vortices in the system, a quantity that is related to the resistance. For $K > K^* = 1/\pi$ the number of free vortices decreases with chain length, while for $K < K^*$ Z_1 decreases with increasing N (a). Corresponding measured resistances. (Reproduced from Ref. 6 with permission.) (b).

tion, which remove the customary logarithmic divergence of E_{typ} .

While the limit $F \rightarrow -\infty$ as $T \rightarrow 0$ is independent of both the coupling constant K and the array length N , the number of free vortices at a particular temperature, and hence the resistance $R(N, T, K)$, depends on N and K as shown in Fig. 2. However, in the limit $N_{\tau} \gg N$, the value of F is roughly independent of the chain length N at a special value of $K = K^* \equiv 1/\pi$, which is different from the critical coupling of the infinite system, $K_{KTB} = 2/\pi^*$. This suggests the possibility of a *length-independent resistance* at this special value of K . Furthermore, in the insulating regime ($K < K^*$), $Z_1 = e^{-F}$ ($\sim R$) increases with increasing array length, while in the superconducting limit Z_1 seems to decrease with chain length (Fig. 2,a). This is indeed what experimentalists report [6]. The observed value of the special coupling $K_{\text{exp}}^* \approx 0.5$ lies in between these two values K_{KTB} and K^* .

The preceding analysis disregards the effect of vortex-antivortex pairs on the free energy of isolated vortices. These pairs partially screen out the spin-spin interactions, hence lowering the energy of vortex configurations, or equivalently, renormalizing the coupling constant to an effective value $K_{\text{eff}}(K) < K$. This effect is more pronounced below K^* , when vortex-antivortex pairs are abundant, effectively bending the curves in Fig. 2,a upwards for small K . However, this argument does not explain why $K_{\text{eff}}(K)$ should reproduce the experimentally observed similar slopes of the different curves in the two regimes separately (Fig. 2,b).

4. Numerical analysis

4.1. Methods

The $\omega \rightarrow 0$ limit of the intrinsic linear-response conductance of the array can be compactly expressed as

$$\sigma_0 = - \frac{1}{i\hbar} \frac{\partial}{\partial \omega} \chi_{jj}^{\text{ret}}(q=0, \omega) \Big|_{\omega=0}. \quad (3)$$

As usual [10], the retarded response function is obtained from the analytic continuation

$$\chi_{jj}^{\text{ret}}(q=0, \omega) = \lim_{i\omega_n \rightarrow \omega+i\delta} \int_0^{\hbar\beta} d\tau e^{i\omega_n\tau} \sum_x \chi_{jj}(x, \tau)$$

of the corresponding temperature Green's function, $\chi_{jj}(x, \tau) = \langle j_{N-x}(\tau) j_N(0) \rangle$. Here $\omega_n \equiv n2\pi/\beta$ denotes the n th bosonic Matsubara frequency and $j_x(\tau) = (2e/\hbar)E_J \sin[\varphi(x, \tau) - \varphi(x-1, \tau)]$ is the local current at (x, τ) .

Using the Wolff algorithm [13], a sequence of equilibrium configurations was generated, from which the desired correlation function could be evaluated. The number of update steps taken was typically of the order of 10^7 .

The problem of analytically continuing imaginary-time Monte Carlo data to real frequencies is notoriously difficult, and sophisticated statistical methods have been developed to deal with it [14]. However, in accordance with earlier work on two-dimensional Josephson junction arrays [15], we have found it sufficient to fit the MC data to a functional Padé-type form that can easily be analytically continued,

$$\chi_{jj}(q=0, i\omega_n) \approx \frac{A}{B\omega_n^2 + C|\omega_n| + 1}.$$

This functional form is motivated by analytic calculations on the superconducting [1] and insulat-

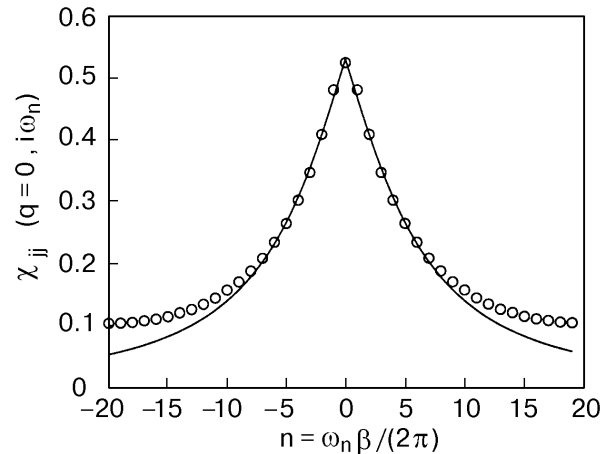


Fig. 3. Example of a Padé-type rational polynomial fit to $\chi_{jj}(q=0, i\omega_n)$ for small Matsubara frequencies. In this particular case, $N = 10$, $N_{\tau} = 40$ and $K = 1.2$. (The correlation function is given in units of the critical current squared, I_c^2).

* A standard finite size scaling argument would imply size-independent behavior at $K = 2/\pi$. However, such an argument applies to *isotropic* rescaling, where both N and N_{τ} are changed.

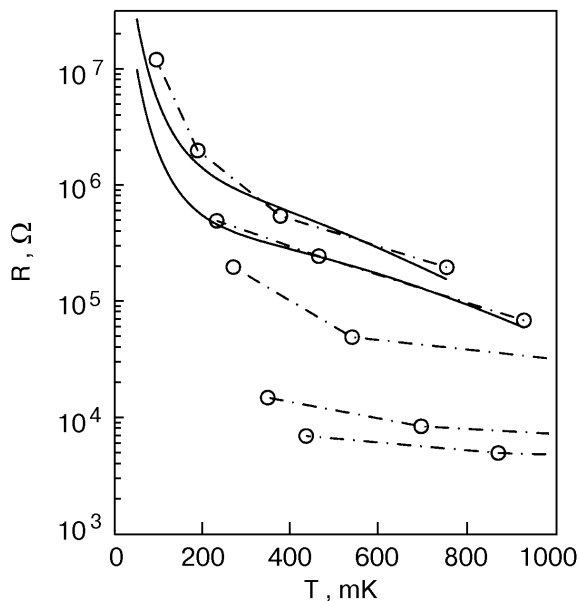


Fig. 4. The resistance obtained from Monte Carlo calculations for a chain of length $N = 10$ (dash-dotted lines are included as a guide to the eye). From top to bottom, the data correspond to $K = 0.65, 0.8, 0.93, 1.2,$ and 1.5 , respectively. The solid lines plot the quantity $R_0(K)[Z_1(K)]^2$ of Section 4.2 for the two lowest values of K . For larger values of K , both MC data and the analytic expression display few features, and a comparison becomes less meaningful.

ing [16] sides of the superconductor–insulator transition in infinite arrays at zero temperature. It has the required symmetry and accurately fits the low-frequency part of the MC data.

4.2. Results

The conductance is now obtained straightforwardly. Conditions for the fitting parameters are imposed by the requirements that the resulting real-time Green’s function be causal, and that the conductance be positive. A typical fit is shown in Fig. 3.

The simulations suffer from noise problems and therefore become quite time-consuming, particularly at low temperatures. This problem becomes rather pronounced, since the dependences we wish to examine typically vary only logarithmically. We were therefore forced to consider only small systems (typically, $N = 10$ and values of N_τ ranging from $N/2$ to $8N$) and to focus on the temperature dependence only. A plot of the resulting resistance, together with the corresponding heuristic result, is shown in Fig. 4. Comparison between the MC data and the heuristic argument (Fig. 4) suggests that the

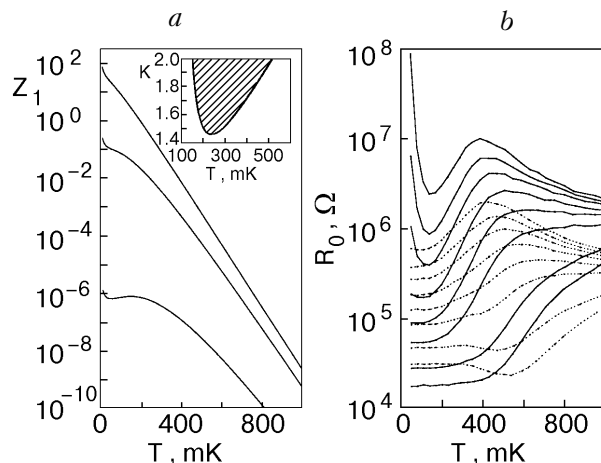


Fig. 5. The quantity Z_1 (\sim number of isolated vortices) for a $N = 63$ chain. The different curves correspond, from top to bottom, to increasing values of the coupling constant $K = \sqrt{E_J/E_C}$ (0.5, 1, and 2, respectively). Inset: «phase diagram» showing regions where $\partial Z_1/\partial T > 0$ (shaded area) for a $N = 20$ array. The location and width of the shaded region both scale as N^{-1} (a). Experimentally measured linear-response resistance vs. temperature, $R(T)$, for two chains of respectively 63 (dashed line) and 255 (solid line) Josephson junctions. From top to bottom in each set of curves, the ratio E_J/E_C increases. (From Ref. 6) (b).

connection between R and Z_1 is roughly $R(K, T) = R_0(K)[Z_1(K, T)]^\alpha$ with $\alpha \approx 2$, where $R_0(K)$ is a coupling-constant-dependent resistance scale.

4.3. Comparison with experiments

In the experiment by Chow et al. [6] the mutual capacitance C_m between grains was much larger than the ground capacitance C_g , and therefore the experiment does not exactly correspond to the self-charging model we have investigated. The $C_m \gg C_g$ case was analyzed by Bradley and Doniach [1], who concluded that C_m -dominated arrays are always insulating in the $T \rightarrow 0, N \rightarrow \infty$ limit, as opposed to C_g -dominated arrays, which become superconducting for large values of E_J/E_C . Consequently, we expect that including nonzero mutual capacitances would result in an increase of the resistance at finite N and T .

The large values of N used in experiments render a direct MC analysis unfeasible; we therefore compare the experiments with the simple analytic estimates in Sec. 3. Figure 5, a shows the estimated number of isolated vortices Z_1 plotted as a function of T for several different values of the coupling constant K . For low values of K , which are consistent with the charging and Josephson energies in

the experiments, we find that Z_1 increases monotonically with decreasing temperature, suggesting a monotonically increasing $R(T)$. For large values of K^* , the number of isolated vortices varies non-monotonically with temperature, reaching a minimum at a low temperature T_{\min} that is roughly independent of K , and exhibiting a local maximum at a higher, K -dependent temperature T_{\max} . This is indicated in the inset of Fig. 5,*a*, where the shaded area corresponds to regions with $\partial Z_1/\partial T > 0$. This is in qualitative agreement with the experimental results by Chow et al. [6] shown in Fig. 5,*b*. However, since this structure appears for very large K and is rather weak, it is not clear that it can be identified with the experimentally observed re-entrant behavior.

5. Conclusions and discussion

We have studied the linear-response resistance of a finite one-dimensional array of Josephson junctions as a function of the array length N and the energy scales E_C , E_J , and $k_B T$. The model we have used is the simplest one that incorporates both charging phenomena and phase coupling between adjacent superconductors. Using a standard mapping onto a two-dimensional XY -model on a cylinder, we can relate the resistance to phase fluctuations or vortices in the XY -model. We have analyzed the model both using analytic approximations and by means of numerical Monte Carlo calculations.

We find that the low-temperature resistance is independent of the array length for $E_J/E_C \approx \approx 1/\pi^2 \approx 0.1$, which can be compared with the experimental value of approximately 0.2. We also conclude, based on analytical and numerical results, that the array becomes highly resistive in the low-temperature limit for all values of E_J/E_C . This is in apparent contradiction with the experiments that indicate a saturation of resistance at low temperatures. However, since the temperature dependence that we find is quite weak (logarithmic), one has to be careful in identifying the measurements at a low but finite temperature as the zero-temperature limit.

The experimentally observed resistance saturation at low temperatures is puzzling and may be due to processes that are not included in our model. A possible explanation is that random background charges result in frustration, hence reducing the charge order and, consequently, the resistance of the array [17]. Resistance saturation may also arise

within the self-charging model as a result of an external coupling such as charge transfer between the array and external electrodes. Since the internal dynamics of the model only leads to logarithmic dependences $F \sim \log(N, 1/T)$, the system is very sensitive to any perturbation that leads to free energy contributions that are linear in $1/T$ and possibly even in N . Such a term arises, e.g., from the coupling between the array and the external electrodes and is expected to affect the behavior of the array in the limit $T \rightarrow 0$. Specifically, if the free energy acquires a form $F \approx -\ln N_\tau + \gamma/T$ (cf. Eq. (3)), the free energy acquires a minimum at $T = \gamma$, and for temperatures $T < \gamma$ the number of free vortices (and hence the resistance) is reduced. It should be possible to determine experimentally if the saturation of the resistance at low temperatures is due to such coupling to the external leads – if this is the case, the saturation temperature should vary with the strength of the coupling.

Acknowledgments

We wish to acknowledge fruitful discussions with, and insightful contributions from, Robert Shekhter, Sebastian Eggert, David Haviland, and Steven Girvin. Financial support was provided by the Swedish Foundation for Strategic Research (SSF) program «Quantum Devices and Nano-Science» and by the Swedish Natural Science Research Council.

1. R. M. Bradley and S. Doniach, *Phys. Rev.* **B30**, 1138 (1984).
2. S. G. Chung, *J. Phys.: Condens. Matter* **9**, L619 (1997).
3. T. Inoue, M. Nishida, and S. Kurihara, *cond-mat/9903349 (unpublished)*.
4. A. I. Larkin and L. I. Glazman, *Phys. Rev. Lett.* **79**, 3736 (1997).
5. M.-S. Choi, J. Yi, M. Y. Choi, J. Choi and S.-I. Lee, *Phys. Rev.* **B57**, R716 (1998).
6. E. Chow, P. Delsing, and D. B. Haviland, *Phys. Rev. Lett.* **81**, 204 (1998).
7. S. L. Sondhi, S. M. Girvin, J. P. Carini, and D. Shahar, *Rev. Mod. Phys.* **69**, 315 (1997).
8. G. Schön and A. D. Zaikin, *Phys. Rep.* **198**, 239 (1990).
9. J. M. Kosterlitz and D. J. Thouless, *J. Phys.* **C6**, 1181 (1973).
10. G. D. Mahan, *Many-Particle Physics*, Plenum, New York (1993).

* Non-monotonicity appears for $K \geq 1.63 - 3.4N^{-1} + O(N^{-2})$.

11. P. M. Chaikin and T. C. Lubensky, *Principles of Condensed Matter Physics*, Cambridge University Press, Cambridge (1995).
12. Similar instanton configurations have been studied by I. V. Krive, P. Sandstrom, R. I. Shekhter, S. M. Girvin, and M. Jonson, *Phys. Rev.* **B52**, 16451 (1995).
13. U. Wolff, *Phys. Rev. Lett.* **62**, 361 (1989).
14. M. Jarrell and J. E. Gubernatis, *Phys. Rep.* **269**, 133 (1996).
15. M. Wallin, E. S. Sorensen, S. M. Girvin, and A. P. Young, *Phys. Rev.* **B49**, 12115 (1994).
16. K. B. Efetov, *Sov. Phys. JETP* **51**, 1015 (1980).
17. C. Bruder, R. Fazio, A. Kampf, A. van Otterlo, and G. Schon, *Phys. Scrip.* **42**, 159 (1992).